Figure S1

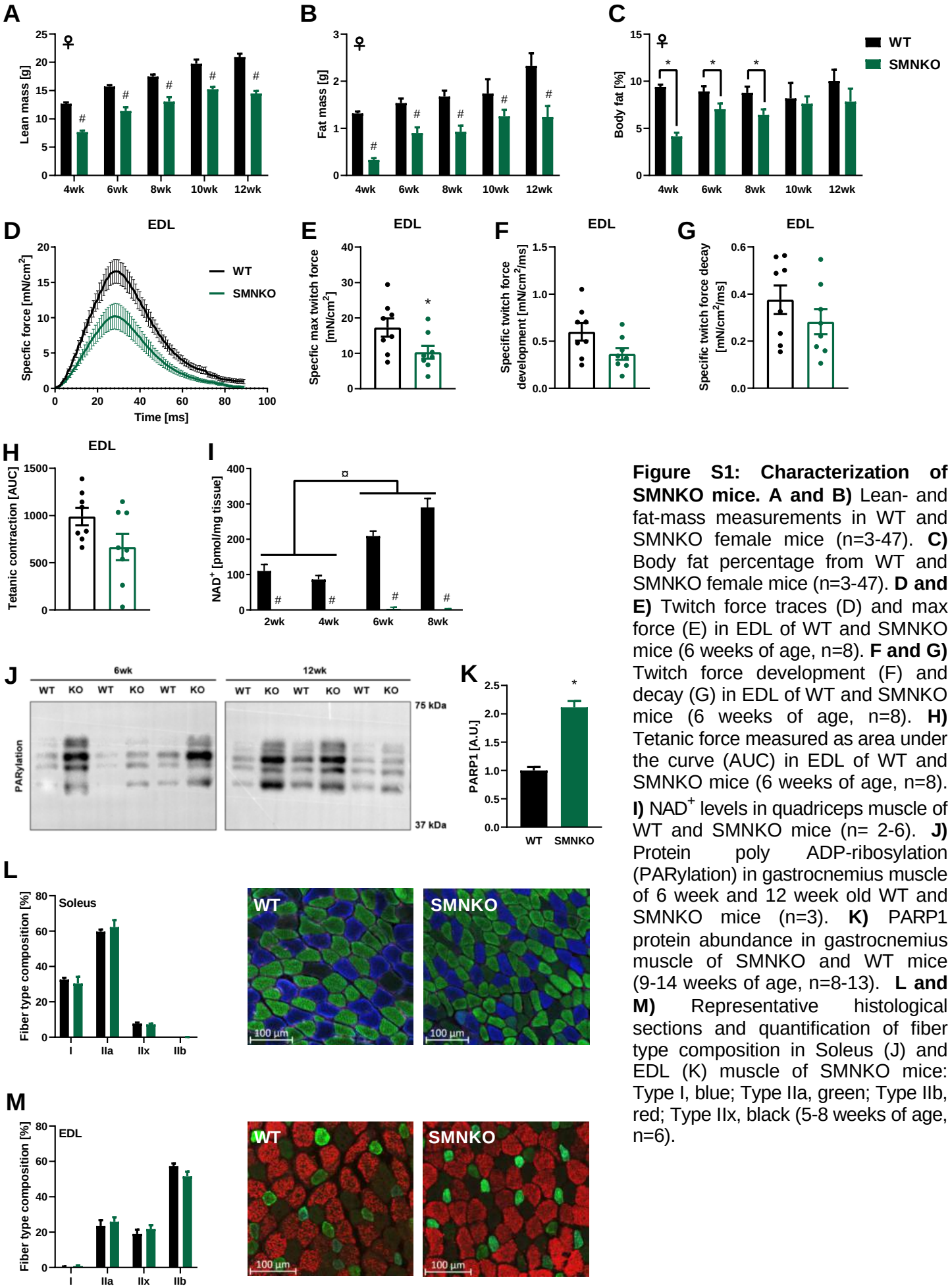

Figure S1: Characterization of SMNKO mice. A and B) Lean- and fat-mass measurements in WT and SMNKO female mice (n=3-47). **C)** Body fat percentage from WT and SMNKO female mice (n=3-47). **D and E)** Twitch force traces (D) and max force (E) in EDL of WT and SMNKO mice (6 weeks of age, n=8). **F and G)** Twitch force development (F) and decay (G) in EDL of WT and SMNKO mice (6 weeks of age, n=8). **H)** Tetanic force measured as area under the curve (AUC) in EDL of WT and SMNKO mice (6 weeks of age, n=8). **I)** NAD^+ levels in quadriceps muscle of WT and SMNKO mice (n= 2-6). **J)** Protein poly ADP-ribosylation (PARylation) in gastrocnemius muscle of 6 week and 12 week old WT and SMNKO mice (n=3). **K)** PARP1 protein abundance in gastrocnemius muscle of SMNKO and WT mice (9-14 weeks of age, n=8-13). **L and M)** Representative histological sections and quantification of fiber type composition in Soleus (J) and EDL (K) muscle of SMNKO mice: Type I, blue; Type IIa, green; Type IIb, red; Type IIx, black (5-8 weeks of age, n=6).

Figure S2

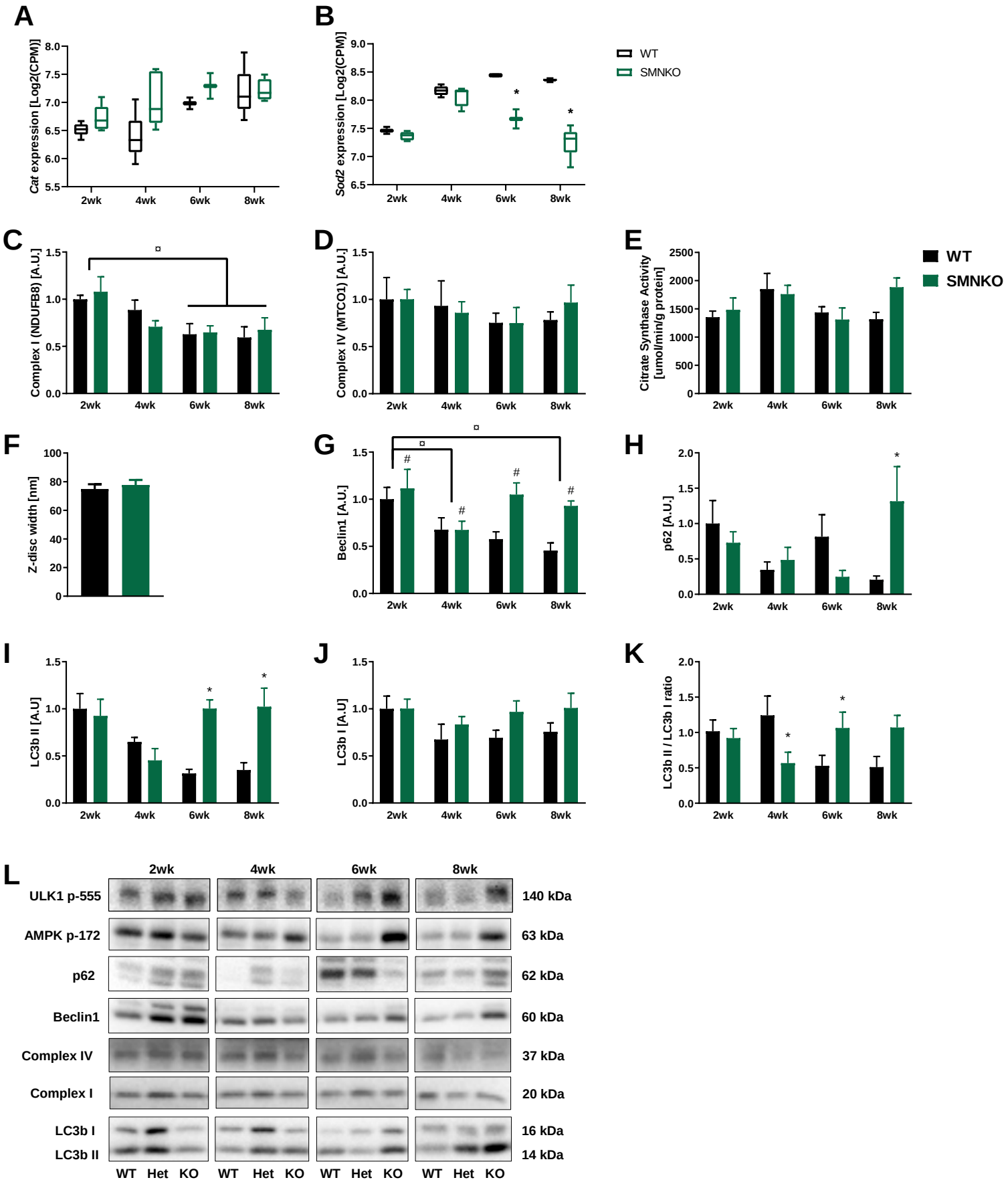

Figure S2: Nampt knockout increases autophagy in skeletal muscle. A and B) Expression of *Cat* (A) and *Sod2* (B) based on RNA sequencing data from gastrocnemius muscle of WT and SMNKO mice (n=2-6). **C and D)** Protein levels of Complex I (NDUFB8) (C) and Complex IV (MTCO1) (D) in quadriceps muscle of WT and SMNKO mice (n= 2-6). **E)** Citrate synthase activity in quadricep muscle of WT and SMNKO mice (n= 2-6). **F)** Quantification of z-disk thickness in quadriceps muscles of WT and SMNKO male mice, (5-8 weeks of age, n=6). **G and H)** Protein levels of Beclin 1 (G) and p62 (H) in quadriceps muscle of WT and SMNKO mice (n= 2-6). **I and J)** Protein levels of LC3b II (I) and LC3b I (J) in quadriceps muscle of WT and SMNKO mice (n= 2-6). **K)** LC3b II/LC3b I ratio in quadriceps muscle of WT and SMNKO mice (n= 2-6). **L)** Representative Western blots of ULK1-pS555, AMPK-pT172, p62, Beclin 1, Complex I (NDUFB8), Complex IV (MTCO1), LC3b I and LC3b II in quadriceps muscle of WT and SMNKO mice at 2, 4, 6, and 8 weeks of age. Error bars represent SEM. * Difference to WT control of the same age. # Main effect of genotype. ¤ Main effect of time.

Figure S3

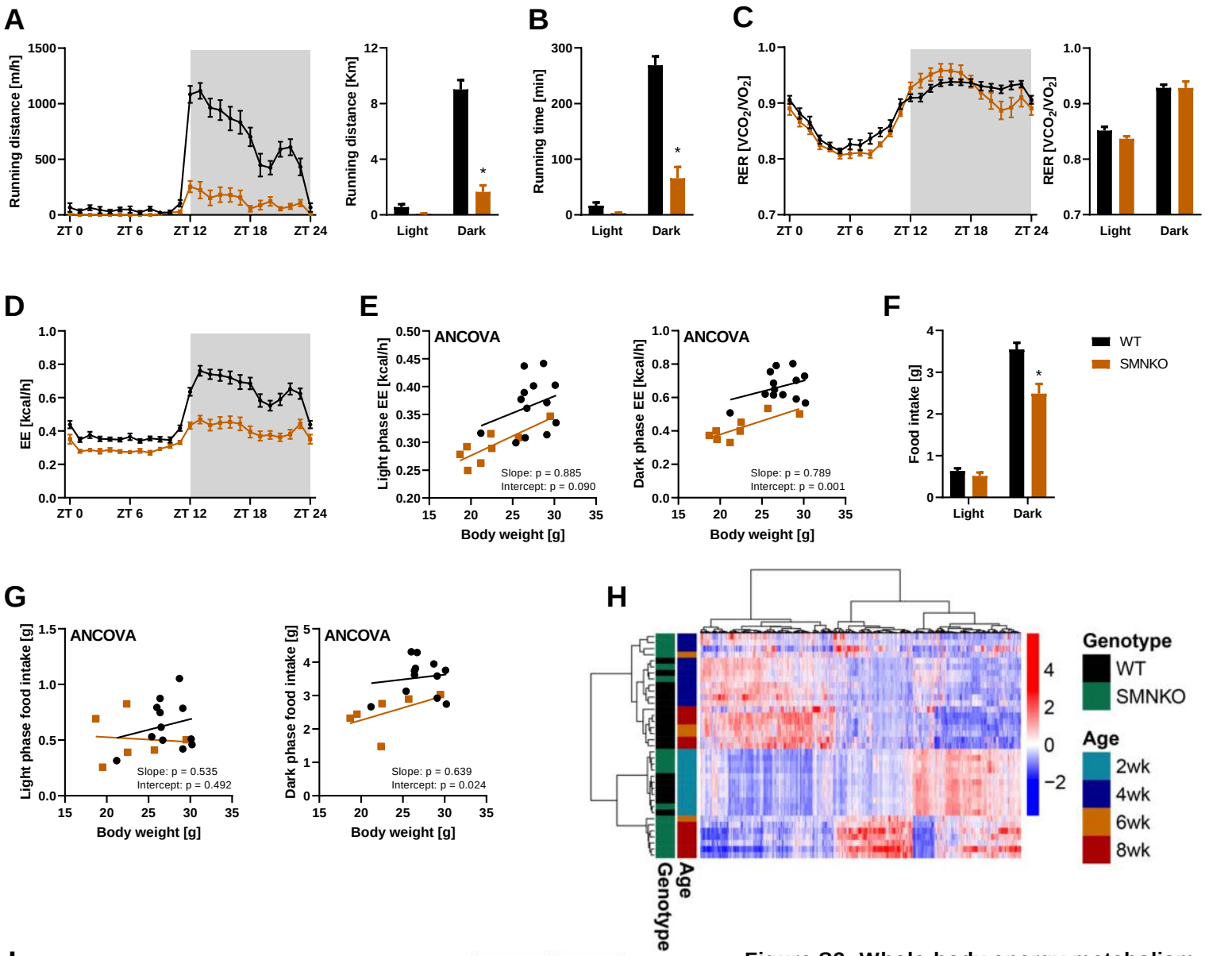

Figure S3: Whole-body energy metabolism and transcriptomic analysis of SMNKO mice. **A)** 24-hours time course of running distance and average running distance in the light and dark phase of WT and SMNKO male mice with access to a running wheel (8-14 weeks of age, n=8-13). **B)** Average running time in the light and dark phase of WT and SMNKO male mice with access to a running wheel (8-14 weeks of age, n=8-13). **C)** 24-hours time course of RER and average RER in the light and the dark phase of WT and SMNKO male mice with access to a running wheel (8-14 weeks of age, n=8-13). **D)** 24-hours time course of EE in the light and the dark phase of WT and SMNKO male mice with access to a running wheel (8-14 weeks of age, n=8-13). **E)** ANCOVA analysis with EE in the light and dark phase as the dependent viable and body weight as a covariant for WT and SMNKO male mice with access to a running wheel, (8-14 weeks of age, n=8-13). The analysis showed that genotype significantly affected EE independently of body weight in the dark phase. **F)** Food intake in the light and the dark phase of WT and SMNKO male mice with access to a running wheel (8-14 weeks of age, n=8-13). **G)** ANCOVA analysis with food intake in the light and dark phase as the dependent viable and body weight as a covariant for WT and SMNKO male mice with access to a running wheel, (8-14 weeks of age, n=8-13). The analysis showed that genotype significantly affected food intake independently of body weight in the dark phase. **H)** Heatmap of RNA sequencing data from gastrocnemius muscle of WT and SMNKO mice at 2, 4, 6, and 8 weeks of age (n= 2-6). **I)** Gene set enrichment analysis of genes differentially expressed between genotypes and separated by age. The biological pathways were manually clustered into main pathways (n= 2-6). Normalized enrichment score (NES). Error bars represent SEM. * Difference to WT control of the same light phase.

Figure S4

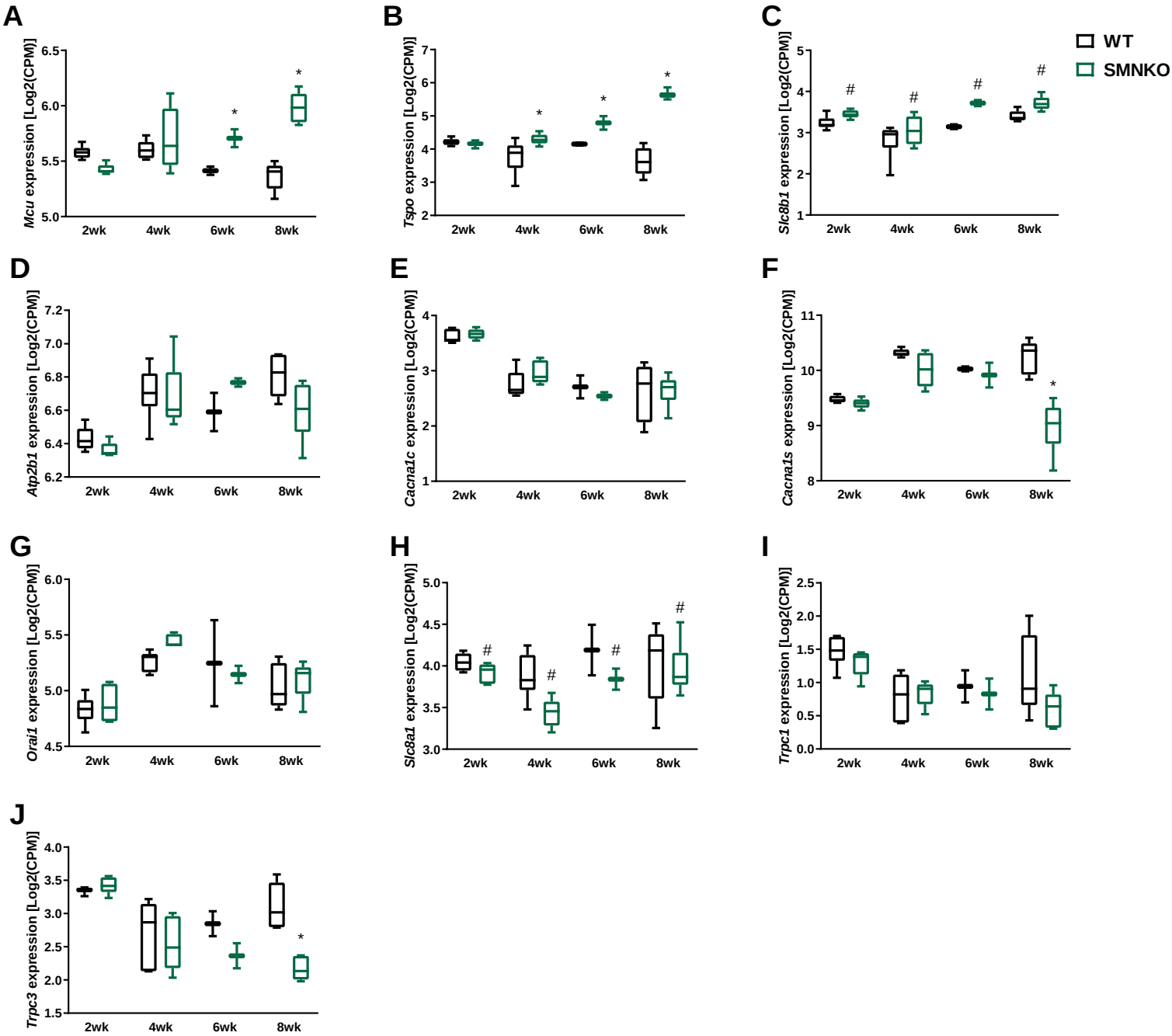

Figure S4: Expression of mPTP related genes and Ca^{2+}-transporters in SMNKO mice. A-C) Expression based on RNA sequencing data of mitochondria permeability transition pore (mPTP) related proteins: Mitochondrial Calcium Uniporter (*Mcu*) (A), Translocator protein (*Tspo*) (B), and Solute Carrier Family 8 Member B1 (*Slc8B1*) (C) on gastrocnemius muscle of WT and SMNKO mice (n= 2-6). **D-J)** Expression based on RNA sequencing data of Ca^{2+}-transporters connected to the sarcolemma: ATPase plasma membrane Ca^{2+} transporting 1 (*Atp2b1*) (D), Ca^{2+} voltage-gated channel subunit α1 C (*Cacna1c*) (E), Ca^{2+} voltage-gated channel subunit α1 S (*Cacna1s*) (F), Ca^{2+} release-activated Ca^{2+} channel protein 1 (*Orai1*) (G), Solute carrier family 8 member A1 (*Slc8a1*) (H), Transient receptor potential cation channel subfamily C member 1 (*Trpc1*) (I), Transient receptor potential cation channel subfamily C member 3 (*Trpc3*) (J) in gastrocnemius muscle of WT and SMNKO mice (n= 2-6). Box plot: boxes extend from the 25th to 75th percentiles and the whiskers represent the smallest to the largest value. * Difference to WT control of the same age. # Main effect of genotype.

Figure S5

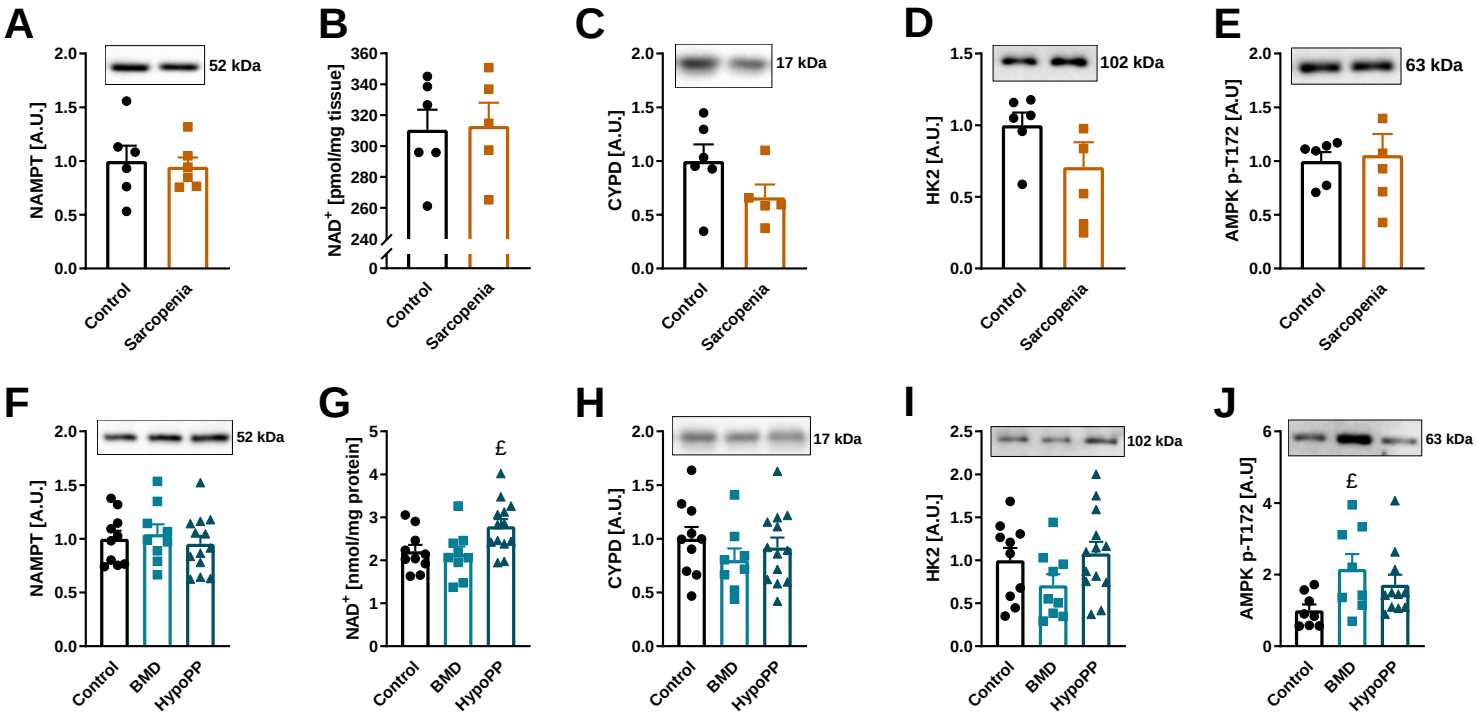

Figure S5: NAMPT and NAD$^+$ levels in human myopathies. A-B) NAMPT (A) and NAD$^+$ (B) levels in human control and sarcopenic muscle (n=5-6) taken from individuals with sarcopenia (age: 85-93 years of age, total appendicular lean mass normalized to height <6.94 kg/m2 for men and <5.33 kg/m2 for women) or from age-matched healthy controls (age: 83-88 years of age, total appendicular lean mass normalized to height >8.16 kg/m2 for men and >5.90 kg/m2 for women). **C-E)** CYPD (C), HK2 (D), and AMPK-pT172 (E) protein levels in human control and sarcopenic muscle (n=5-6). **F-G)** NAMPT (F) and NAD+ (G) levels in muscle biopsies of controls and patients with Becker muscular dystrophy (BMD) or Hypokalemic periodic paralysis (HypoPP) (n= 9-13). **H-J)** CYPD (H), HK2 (I), and AMPK-pT172 (J) protein levels in muscle biopsies of controls and patients with Becker muscular dystrophy (BMD) and Hypokalemic periodic paralysis (HypoPP) (n= 9-13). Error bars represent SEM. £ p<0.05 compared to controls.

Figure S6

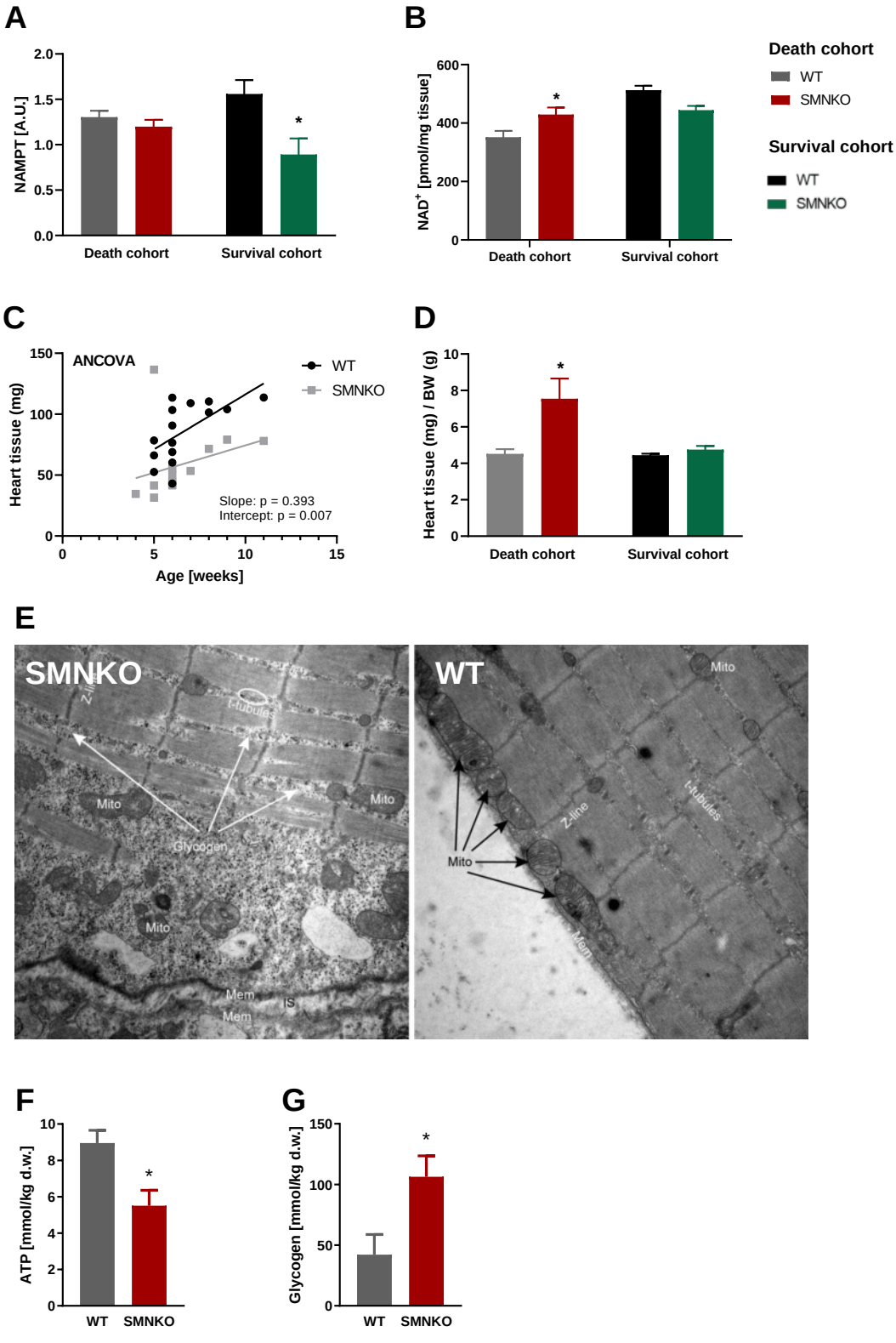

Figure S6: Glycogen accumulation in SMNKO muscle. A and B) NAMPT protein abundance (A) and NAD^+ levels (B) in cardiac tissue of WT and SMNKO mice sacrificed just before natural death of the SMNKO mice (Death cohort, 4-11 weeks of age, n= 15), and in male WT and SMNKO mice (Survival cohort, 9-14 weeks of age, n= 8-13). **C and D)** Heart tissue weight as a function of age (C) and heart tissue weight normalized to bodyweight (D) in WT and SMNKO mice (Death cohort, 4-11 weeks of age, n= 15 and Survival cohort, 9-14 weeks of age, n= 8-13). **E)** Left: Glycogen accumulates in the subsarcolemmal space, between and in the interior of myofibrils from SMNKO mice causing them to break up longitudinally, splitting the Z-line (IS: interstitial space between myofibers; Mem: membrane; Mito: mitochondria. White arrows: glycogen; Black arrows: mitochondria). Right: Myofibrils from WT muscle. **F)** ATP and **G)** glycogen levels in diaphragm muscle of WT and SMNKO mice sacrified just before natural death of the SMNKO mice (Death cohort, 4-11 weeks of age, n=11).

Supplementary Table 1

SYMBOL	FULL NAME	P-VALUE	FDR	DIRECTION	FUNCTION
Gm10800	Predicted gene 10800	2,39E-13	3,59E-09	Up (wk: 2, 4, 6, 8)	Unknown
Nampt	Nicotinamide phosphoribosyl-transferase	6,59E-11	4,96E-07	Down (wk: 2, 4, 6, 8)	Enzyme in the NAD salvage pathway.
Gm10801	Predicted gene 10801	2,14E-10	1,07E-06	Up (wk: 2, 4, 6, 8)	Unknown
Chrna9	Cholinergic receptor, nicotinic, alpha polypeptide 9	9,19E-07	0,00346	Up (wk: 2, 4, 6, 8)	Ligand-gated plasma membrane channel for divalent cations. B and T cell related.
Gm5083	Predicted gene 5083	1,38E-06	0,00348	Up (wk:2)	Unknown
Gm21738	Predicted gene, 21738	1,39E-06	0,00348	Up (wk: 2, 4, 6, 8)	Unknown
Acsl4	Acyl-CoA synthetase long-chain family member 4	2,27E-06	0,00489	Down (wk: 2, 4)	Convert arachidonate into fatty acyl-CoA esters. Regulates PGE_2 release.
Rps6ka6	Ribosomal protein S6 kinase polypeptide 6	1,31E-05	0,02473	Down (wk:2)	Constitutively active growth-factor-independent kinase.
Rnf128	Ring finger protein 128	1,69E-05	0,02834	Down (wk: 2, 4, 6, 8)	Involved in the endocytic pathway. Related to anergic T cells.
Ppif	Cyclophilin D	3,28E-05	0,04542	Up (wk: 2, 4, 6, 8)	Major component of the mitochondrial permeability transition pore.
Pter	Phosphotriesterase related	3,32E-05	0,04542	Down (wk: 2, 4, 8)	Mediates renal injury in response to urinary protein.

Supplementary Table 2

Content of purified NR enriched diet.

Composition	**Grams**	**Kcal %**
Protein	19	20
Carbohydrate	67	70
Fat	4	10
Total		100
Calorie/gram	3.8	
Ingredients	**Grams**	**Kcal**
Casein	200	800
L-cysteine	3	12
Corn starch	506.2	2025
Maltrodextrin 10	125	500
Sucrose	68.8	275
Cellulose, BW200	50	0
Soybean oil	25	225
Lard	20	180
Mineral mix S10026	10	0
Dicalcium phosphate	13	0
Calcium carbonate	5.5	0
Potassium citrate, $1H_2O$	16.5	0
Vitamin mix V10001	10	40
Choline bitartrate	2	0
Nicotinamide riboside	1	2
Total	1056	4057